ELSEVIER

Thermochimica Acta 267 (1995) 297–311

thermochimica acta

# Freezing-in phenomena of high-temperature structures and their structural determination for henpentacontane and dopentacontane[1]

Kanichiro Takamizawa[a], Yoshiko Urabe[a,*], Jyuichi Fujimoto[a], Hidetake Ogata[a], Yoshihiro Ogawa[b]

[a]*Department of Applied Science, Faculty of Engineering, Kyushu University, Hakozaki, Higashi-ku, Fukuoka 812, Japan*

[b]*Department of Chemistry, Faculty of General Education, Kumamoto University, Kurokami, Kumamoto 860, Japan*

Received 13 January 1995; accepted 24 February 1995

## Abstract

Pure henpentacontane (C51) and dopentacontane (C52) were synthesized. Solution-crystallized samples of both *n*-alkanes clearly showed solid-solid phase transition peaks on their DSC curves before melting, while melt-crystallized samples did not show these peaks. From X-ray and SEM observations, this phenomenon was ascribed to the fact that the high-temperature structures were frozen during crystallization from the melt. By solution crystallization at a temperature range in which the high-temperature phase exists in bulk crystals, single crystals consisting of the high temperature structures were obtained. In X-ray diffraction, the lattice parameters for C51 were determined from Weissenberg photographs, and that of $P2_1/a$ for C52, from oscillation observations. It was noted that the even-odd effect of the number of carbon atoms still works with the high-temperature structures.

*Keywords:* Henpentacontane; Dopentacontane; High-temperature structures; Freezing-in

## 1. Introduction

Studies on higher *n*-alkanes (C*n*, where *n* is the number of carbon atoms in a chain) have been useful for understanding the properties of perfectly crystalline polyethylene. Much work has been done in order to elucidate the structural features and transition be-

---

[*] Corresponding author.

[1] Presented at the 30th Anniversary Conference of the Japan Society of Calorimetry and Thermal Analysis, Osaka, Japan, 31 October–2 November 1994.

*SSDI* 0040-6031 (95) 02487-5

havior of the *n*-alkanes. Our previous work indicated that the odd *n*-alkanes from C45 to C69 showed solid-solid phase transition before melting in which the orthorhombic subcell remained unchanged [1]. The structures of the high-temperature modifications of C33 were also reported [2]. The highest-temperature phase (C) below the hexagonal phase had an oblique structure in which the chain axis inclined 106.5° with respect to the end methyl plane [2]. It was assumed that the high-temperature modifications observed for the higher odd *n*-alkanes had the same type of structure as C33. Similar solid-solid transition was also observed in the even *n*-alkanes of C48 and C60 [1]. Up to the present, details of the oblique structure of even *n*-alkanes were unknown. It is necessary to note here that for higher *n*-alkanes up to C69 the transition to oblique structures is first-order [1].

Characterization of these high-temperature structures and elucidation of the mechanism of the phase transitions are important, since they provide a means of predicting the melting and crystallization behavior of the *n*-alkanes and polyethylene. The appearance of these solid-solid transitions strongly depends on the homologous impurities in the samples used [3,4]. We have continued to produce long *n*-alkanes of purity much higher than those used in Ref. [1]. The present study concerns the freezing-in phenomena of the high-temperature structures of henpentacontane (C51) and dopentacontane (C52). Samples grown from solutions at low temperatures showed phase transitions on their DSC curves before melting, while corresponding peaks were not observed with the melt-crystallized samples. This phenomenon could be interpreted as a result of the freezing-in mechanism of high-temperature structures.

Utilizing freezing-in phenomena, we obtained single crystals with high-temperature structures by solution-crystallization at a temperature within the range in which the high-temperature phase exists in bulk. In addition, the effect of even or odd number of the carbon atoms in long *n*-alkanes on the high-temperature structure is discussed. An oblique structure of a bulk-crystallized sample of tetranonacontane (C94) was briefly reported by Wyckoff et al. [5]. The present study provides further details of these high-temperature structures.

## 2. Experimental

### 2.1. Materials

C51 was synthesized by the following procedure. From icosanoic acid chloride and 1-morpholino-1-cyclohexene, hexacosanoic acid (I) was obtained according to the method of Hunig et al. [6]. **I** free of homologue was obtained by purifying the methyl ester of **I** with preparative liquid chromatography, in which an ODS column was used [4]. Ketene dimerization of the acid chloride of **I** and consecutive hydrolysis resulted in the formation of 26-henpentacontanone, which was then reduced to C51 by Wolff-Kishner's method. Detailed descriptions of the reactions for shorter odd *n*-alkanes were given previously [3,4]. In the present study the dimerization reaction had to be carried out at a relatively high temperature because of the low solubility. This resulted in a side reaction, in which 0.2% C50 and an unknown higher compound were produced. The latter was removed by treatment with hot sulfuric acid (100–115°C). The homologous purity of the C51 sample was determined to be 99.4% by capillary gas chromatography. The starting reagents used were from Sigma.

C52 was synthesized through a Blase-ketone reaction of the dichlorides of icosanedioic acid and *n*-hexadecyl bromide and consecutive reduction was carried out according to the method of Reinhard-Dixon [7]. Icosanedioic acid (purchased from the Okamura Seiyu Co.) was purified as methyl ester by repeated molecular distillation and recrystallization. The bromide purchased (Tokyo Chemical Industry Co. Ltd.) was purified by repeated vacuum distillation. The purity of the C52 sample was 99.8% after treatment with hot sulfuric acid.

Homologous purity was determined by a Shimadzu GC14A capillary gas chromatograph equipped with a column of SGE 25A Q5-HT-5-0.15. Analysis was performed under a heating rate of 1 K $\text{min}^{-1}$ over 330–360°C.

### 2.2. Measurements

DSC measurements were performed by a Rigaku DSC-8240B with a TAS 100 controller. The standard scanning rate of 0.5 K $\text{min}^{-1}$ and sample mass of about 1.00 mg were used. Temperature calibration was performed by using indium (In) and shorter *n*-alkanes, whose equilibrium melting points were determined by a capillary method [8]. The heat of transition ($\Delta H$) was calibrated using In and gallium (Ga).

X-Ray diffraction measurements of single crystals were performed with a Rigaku Weissenberg camera CN 1563A 2. The temperature variation of the long spacing of the solution-crystallized samples was measured with a Rigaku Geigerflex 2027 diffractometer. Both experiments were performed with Ni filtered Cu$K\alpha$ radiation. The radius of the camera was calibrated by the reflections of NaCl. In order to prevent a displacement of the surface of the single crystal mats within the hollow of the glass sample-plate during the heating involved with the diffractometric experiments, the sample was fixed using a thin Be plate. From the Bragg angles, $\theta$, of observed $0\,0\,l$ reflections, the weighted average of $c^*$ was calculated using the following equation:

$$c^* = 2\frac{\sum l \sin\theta / \cos^2\theta}{\sum (l/\cos\theta)^2}$$

This equation was derived by a non-linear least square method in which the reciprocal of $\cos^2\theta$ was taken as the weight.

SEM observation was performed with a JEOL JSM-T100, and Au sputtering on the samples with a JFC-1100E.

## 3. Results and discussion

### 3.1. Thermal analysis and temperature variation of the long period

DSC curves of the C51 samples crystallized from a 0.1% heptane solution are shown

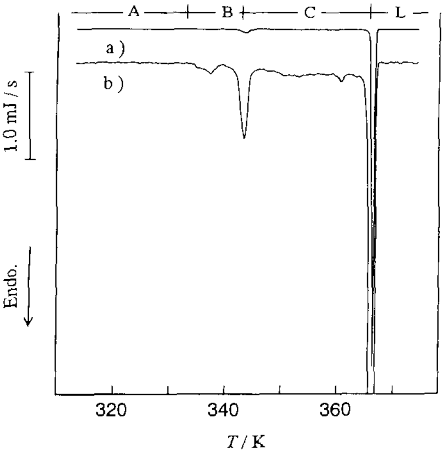

Fig. 1. DSC curves of solution-crystallized samples of henpentacontane (C51): heating rate 0.5 K $\mathrm{min}^{-1}$, sample mass 1.00 mg. (a) Normal drawing; (b) enlarged about 15 times.

in Fig. 1 (the magnification of the ordinate of the lower curve is about 15). The curves elucidate the weak solid-solid transition peaks. These may be ascribed to the transition from the orthorhombic structure (A phase) via a monoclinic structure of the space group $A_a$ (B phase) to that of the space group $A2$ (C phase). This transition is similar to that found previously with C33 [2]. The crystal structure of the C phase is discussed later. At the top of the figure the notation of the phases is given. The thermodynamic data of these phase transitions are listed in Table 1. The very small peak which appears just before melting may be ascribed to kinetic factors rather than to a first order phase transition [9].

Fig. 2 shows the temperature variation of the long spacing, $L$. The values of $L$ correspond to half of the 0 0 $l$ spacing of the orthorhombic and the high-temperature oblique

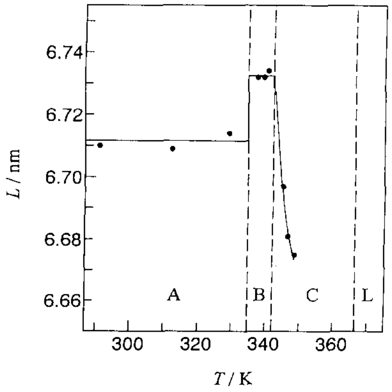

Fig. 2. Temperature dependence of the long period, $L$ (in nm) of solution-crystallized samples of henpentacontane (C51). The dotted lines correspond to the transition temperatures determined by DSC.

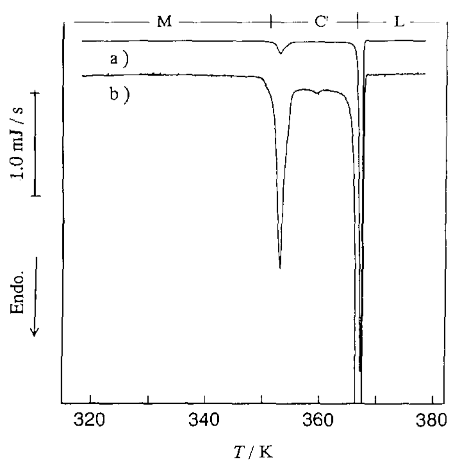

Fig. 3. DSC curves of solution-crystallized samples of dopentacontane (C52): heating rate 0.5 K $\text{min}^{-1}$ sample mass 1.00 mg. (a) Normal drawing; (b) enlarged about 15 times.

forms. The dotted lines indicate the transition temperatures as determined by DSC. In the transition to the B phase the value of *L* slightly increases. This is due to the introduction of disorder in the end methyl zone. A sudden decrease in *L* was observed in passing to the C phase region. In addition the area of the diffraction peak was reduced. Above 350 K the reflection could not be observed. This phenomenon appeared to be caused by the deviation of the reciprocal *c* axis from the initial direction to normal to the sample plate. A simplified representation of the oblique structure is given according to the Sullivan-Weeks notation [10], that is, the Miller subcell index of the terminal end methyl plane. The C phase structure is represented as M101. The calculated value of *L* for M101 is about 6.32 nm. It is located outside the ordinate scale.

The sample of C52 was crystallized from a 0.3% heptane solution as a monoclinic $P2_1/a$. DSC curves of C52 are shown in Fig. 3. The solid-solid transition peaks are very sharp compared to those of C51. The thermodynamic data are compared with those of C51 in Table 1. When the heats of transition are compared in terms of the $CH_2$ unit it suggests that the low-temperature monoclinic form of the even *n*-alkanes is more stable

Table 1

Thermodynamic data of solution-grown crystals of henpentacontane (C51) and dopentacontane (C52)

| | C51 | | | C52 | |
|---|---|---|---|---|---|
| Transitions | A→B | B→C | Melting | M→C′ | Melting |
| *T*/K | 337[a] | 342.1 | 365.7 | 351.8 | 366.7 |
| $\Delta H/k$ J $\text{mol}^{-1}$ | 1.7 | 6.9 | 175.5 | 22.1 | 185.4 |

[a] This transition temperature was determined from the peak position. Other transition temperatures were read from the intersection temperature of the peak front.

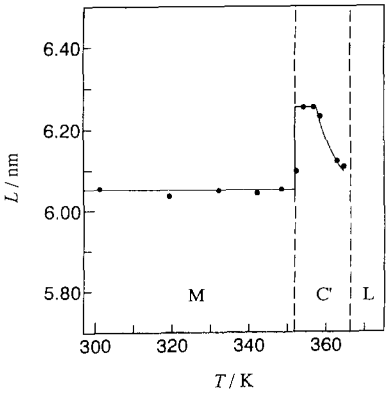

Fig. 4. Temperature dependence of the long period, $L$ (in nm) of solution-crystallized samples of dopentacontane (C52). The dotted lines correspond to the transition temperatures determined by DSC.

than the orthorhombic form of the odd *n*-alkanes. In the case of C52, a small peak also appears in the region of the high-temperature phase.

We would like to point out the effect of the homologous impurity on crystalline forms, as sometimes noted [11]. The C52 sample was very high pure, and the monoclinic crystal was easily prepared. This was in contrast to the previous observation on the C48 sample [1]. The coexistence of the orthorhombic form in the C48 samples could be ascribed to the effect of homologous impurities. A reexamination of its purity using capillary gas chromatography with a higher resolving power resulted in a little lower value of 98.4% compared to the previously reported 99.9% [1]. The purities of almost all the samples shown in Ref. [1] should be decreased by about 2%.

Fig. 4 shows the temperature dependence of the long period $L$. In passing to the high-temperature phase, $L$ slightly increases. With a further increase in temperature, the long period $L$ again decreases. Similar complicated changes in $L$ were also observed for C48 [1]. This suggests that the high temperature phase cannot be unequivocally defined. However, the structure of the crystal, corresponding to the high-temperature structures of the crystals, grown at a high-temperature from a solution, was determined and is discussed later. Despite this ambiguity, we denote the high-temperature oblique structure as the crystal showing the first order transition irrespective of the even or odd number of carbon atoms in the chain.

There is a question whether the phase transition, in which the subcell structure remains unchanged, proceeds reversibly or not. This can be examined by comparing the DSC curves of the solution-crystallized samples of C51 and C52 in Figs. 1 and 3 with those of the bulk-crystallized samples depicted in Fig. 5. The crystallization was performed at a cooling rate of 1 K $h^{-1}$. On the DSC curve for C51, a transition peak to C phase was not found. This feature can be interpreted as a result of the high-temperature oblique structure being frozen-in during the cooling process of the crystallization.

On the DSC measurement, the samples melted directly from the high-temperature phase without any indication of a solid-solid phase transition. On the other hand, the situation for C52 is more complicated. The transition peak did not disappear, and instead

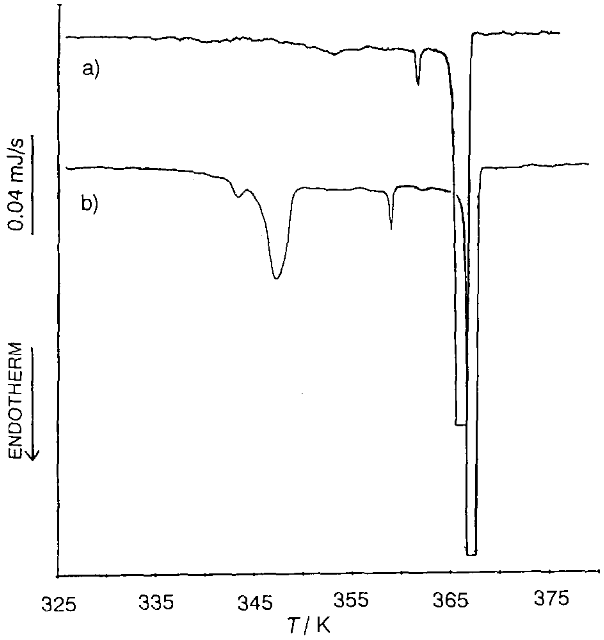

Fig. 5. Comparison of enlarged DSC curves of bulk-crystallized samples of: (a) henpentacontane (C51) and (b) dopentacontane (C52).

of that a smaller and broader peak was observed at about 7 K below the initial peak temperature (Fig. 3). It may be asserted that the recovery to the room-temperature monoclinic form is very difficult, although at present details of this frozen structure is unknown. There is a possibility that the difference in the freezing-in behavior reflects the stability of the crystals of the even-and odd-numbered *n*-alkanes.

As early as 1959, Ohlberg had reported that even-numbered *n*-alkanes showed metastable crystalline forms when crystallized in bulk, and that the metastable forms of the orthorhombic and M101 for pure hexatriacontane (C36) transformed to the equilibrium monoclinic crystal after 3 years [12]. According to our experiment, a sample of C36 with a purity of 99.9% was crystallized in bulk at a cooling rate of 1 K $h^{-1}$ in the equilibrium monoclinic form [13]. It seems that the sample purity and cooling rate, in addition to the chain length, play important roles in the freezing-in phenomena of bulk crystallization. Khoury reported the morphological features of an oblique structure of tetranonacontane (C94) frozen-in during crystallization from the melt [14].

These freezing-in phenomena are further confirmed by the DSC curves of annealed solution-grown crystals. Fig. 6 depicts the DSC curves of C51 crystals annealed at various temperatures. The annealing time was 30 min. Although only a weak peak is discernible, it may be said that most of the high-temperature structure was frozen. The effect of the annealing temperature suggests that the high-temperature phase could not be unequivocally defined.

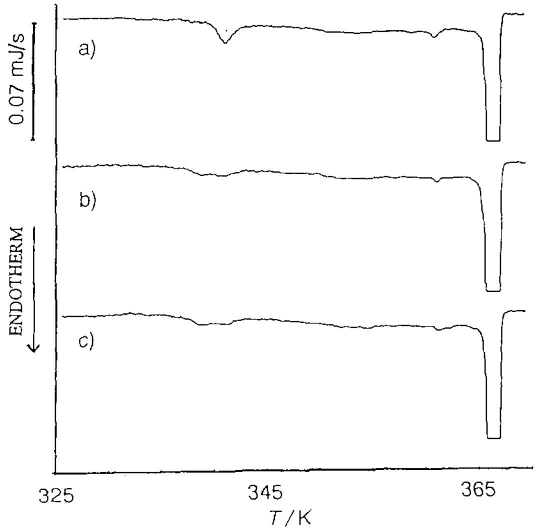

Fig. 6. DSC curves of annealed samples of solution-crystallized henpentacontane (C51). Annealing temperatures: (a) 345 K; (b) 355 K; (c) 363 K. Annealing time: 30 min.

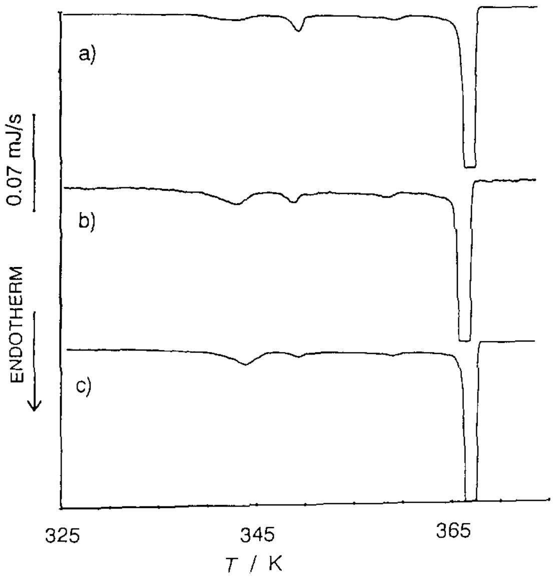

Fig. 7. DSC curves of annealed samples of solution-crystallized dopentacontane (C52). Annealing temperatures: (a) 356 K; (b) 359 K; (c) 362 K.

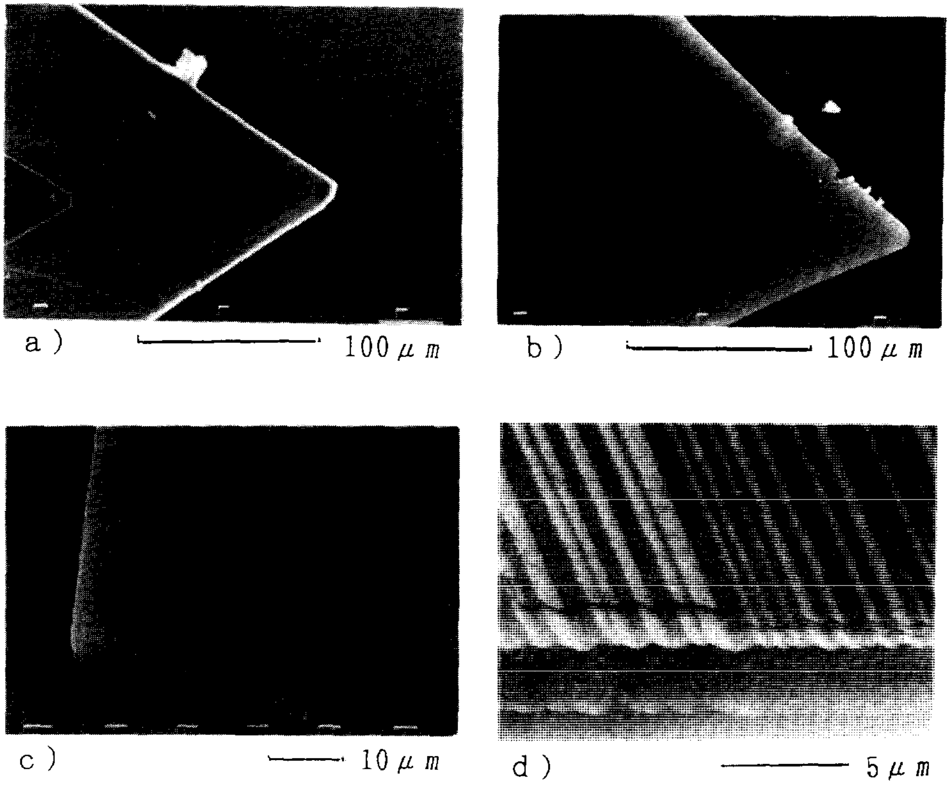

Fig. 8. SEM photographs of solution-crystallized henpentacontane (C51) (a), and annealed solution-crystallized C51 (b), (c), (d). Annealing temperature: 355K. (c) and (d) were taken with an incident angle of 45°.

The annealing effect on the DSC curves of C52 solution-grown crystals is shown in Fig. 7. Being similar in appearance to C51, it can be said that most of the high-temperature structure was frozen.

### *3.2. SEM observation of annealed single crystals*

The freezing-in phenomena were also morphologically confirmed with SEM observations. The photographs in Figs. 8 and 9 are of C51 and C52, respectively. Photo (a) of Fig. 8 shows an as-grown single crystal of C51 (an *a*-axis tip of a lozenge shaped crystal). It seems that the surface of the crystal is smooth. Photos (b) and (c) show crystals annealed at 355 K. The former was taken in a horizontal position and striations along the *b* axis were observed. The fact that the striations consist of ridges of the twined crystals is clearly recognized in photo (c) taken at an inclined position of 45°. Photo (d) taken at a higher magnification clearly indicates that the end methyl plane is inclined by about 20° to the plane of the chain axis. This angle approximately corresponds to that determined

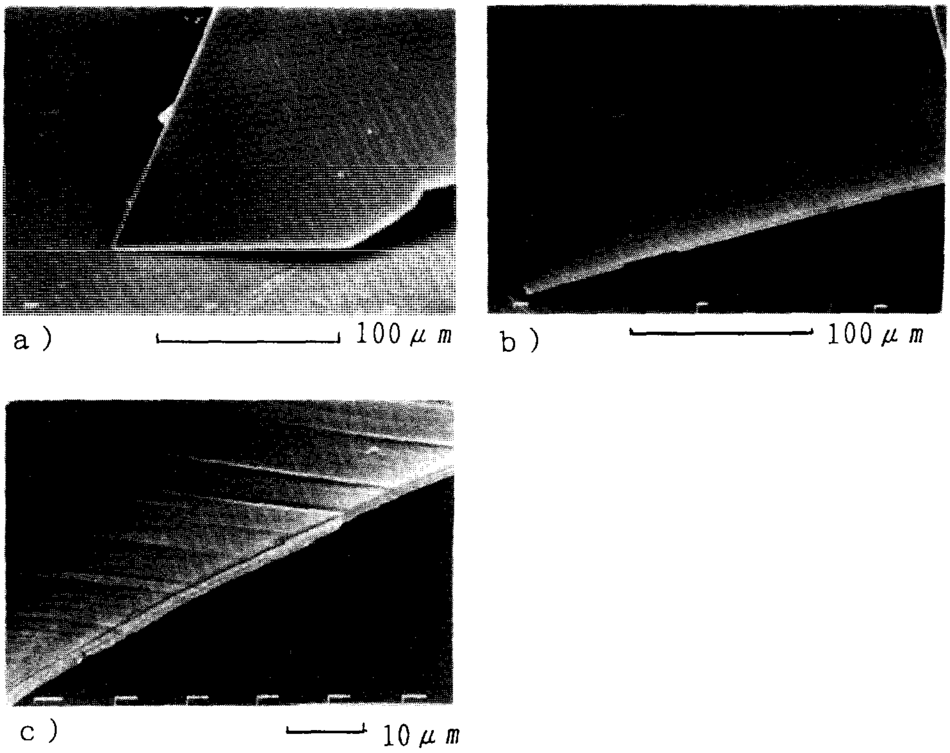

Fig. 9. SEM photographs of solution-crystallized dopentacontane (C52) (a), and annealed solution-crystallized C52 (b), (c). Annealing temperature 359.2 K. (a) was taken with an incident angle of 50°.

for C33 [2]. The distances between ridges is relatively homogeneous and an averaged value is about 0.8 μm. If the solid-solid transition proceeds by a mechanism of nucleation and growth, just like crystallization, and nuclei are formed from defects, this homogeneity of the ridged structure suggests that defects are distributed uniformly and that their density is relatively high.

Similar morphological change by annealing was also observed in C52 single crystals grown from a heptane solution at a low temperature. The smooth surface of the as-grown crystal changes to a striated surface (Fig. 9a) after annealing at 359.2 K for 30 min. Another characteristic morphology is shown in Fig. 9b. Annealing at a relatively low temperature (355.7 K) resulted in a variety of morphological changes; some crystals seemed to be unchanged but other, relatively thin crystals, showed a striated structure.

### *3.3. Determination of the structures of C51 and C52*

The C51 crystals of the stabilizing modification at the high-temperature were grown from a 0.1% *n*-propanol solution by evaporation at 347 K. Their DSC curves did not reveal the solid-solid transition peak before melting (Fig. 10a). It could be said that the

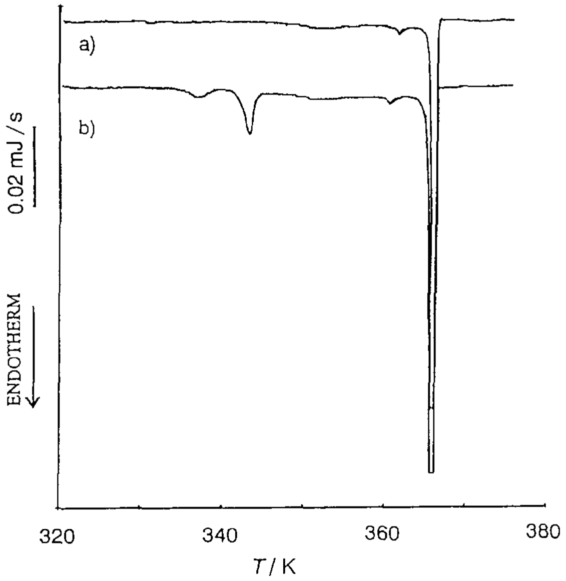

Fig. 10. DSC curves for the solution-crystallized henpentacontane (C51) from *n*-propanol solution at the high-temperature phase region, compared with the room-temperature modification. (a) 347 K; (b) slow cooling to room temperature (heptane solution).

crystals had the high-temperature structure. Good single crystals shown in the SEM photograph of Fig. 12a enabled us to take the rotation, oscillation and Weissenberg photographs. The reflection conditions were $h\ 0\ l$, $h = 2n$ and $0\ k\ 0$, $k = 2n$. The lattice parameters are listed in Table 2. The values reported on the C structure of C33 are as follows: $a = 0.802$ nm, $b = 0.4985$ nm, $c = 8.80$ nm and $\beta = 106.5°$, and the space group is $A2^2$. The monoclinic angle of the C51 crystal differed from that of C33. The reflection patterns for the C51 crystal are similar to those of the C52 high-temperature structure, as described below.

With the C52 samples, initially the stabilizing modification at room temperature were

Table 2

Lattice parameters of C51 (HTP)[a] compared with those of C51 (LTP)[b] Tc = 347 K

| | HTP | | LTP |
|---|---|---|---|
| *a* (nm) | 0.904 | *a* (nm) | 0.744 |
| *b* | 0.496 | *b* | 0.496 |
| *c* | 13.52 | *c* | 13.42 |
| $\beta$ (°) | 125.6 | | |
| Space group | *Pcam* | Space group | $P2_1/a$ |

[a] High temperature phase.
[b] Low temperature phase.

Table 3

Lattice parameters of C52 (HTP) $T_c = 353$ K compared with those of C52 (LTP)

| | HTP | | LTP |
|---|---|---|---|
| | Type 1 | Type 2 | |
| *a* (nm) | 0.736 | 0.904 | 0.557 |
| *b* | 0.496 | 0.496 | 0.742 |
| *c* | 6.857 | 6.896 | 6.885 |
| $\beta$ (deg) | 93.1 | 125.6 | 118.8 |
| Space group | $P2_1/a$ | $P2_1/a$ | $P2_1/a$ |

examined from photographs about the *a* and *b* axes. Relatively good crystals were grown at room temperature in a jar, by slow cooling a 0.1% heptane solution. The reflection conditions were: *h 0 l*, $h = 0$; *0 k 0*, $k = 0$. The long spacing was determined from the oscillation photograph. The lattice parameters and space groups are listed in Table 3. These show that the room-temperature C52 crystal is isomorphous to the monoclinic hexatriacontane (C36) reported by Shearer and Vand [11] ($a = 0.557$ nm and $b = 0.742$ nm and the monoclinic angle $\beta = 119.6°$).

The C52 crystals of the stabilizing structure at high-temperature were grown from a

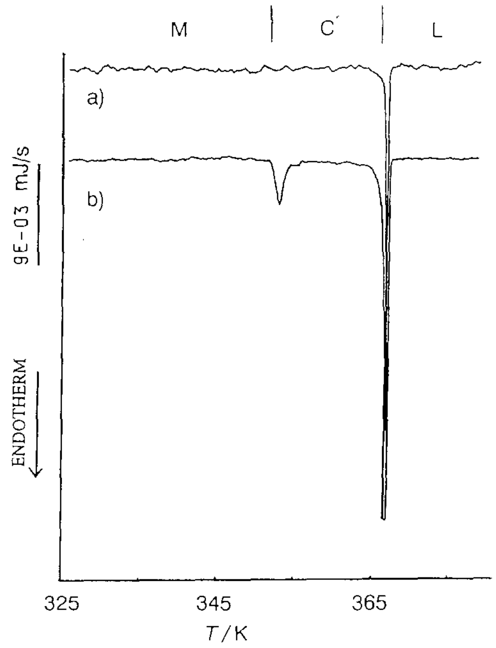

Fig. 11. DSC curves for the solution-crystallized dopentacontane (C52) from *n*-propanol solution at high-temperature phase region, compared with the room-temperature modification. (a) 353 K; (b) slow cooling to room temperature (heptane solution).

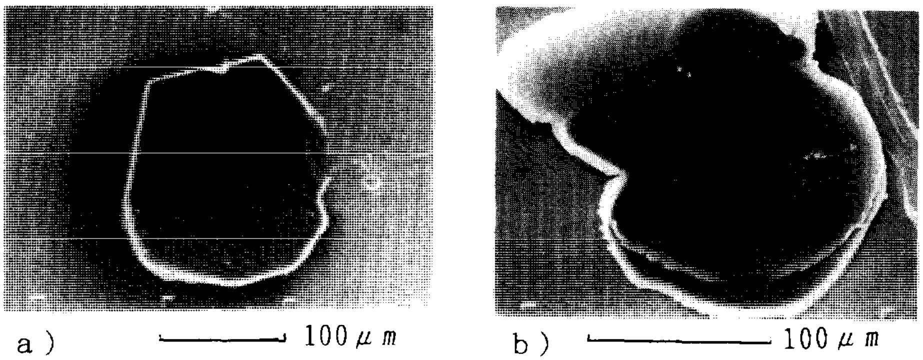

Fig. 12. SEM photographs for the solution-crystallized sample from *n*-propanol solution at the high-temperature phase region, (a) C51, 347 K; (b) C52, 353 K.

0.2% *n*-propanol solution by evaporation at 353 K. Their DSC curve also indicated the freezed-in high-temperature structure (Fig. 11a). The SEM photograph of the crystal is shown in Fig. 12b in which the striated structure along the *b* axis was not observed. The crystals showed good orientation and Weisenberg photographs were taken. The reflection conditions were: *h 0 l*, $h = 2n$ and *0 k 0*, $k = 2n$. The results indicated that two types of unit cells were presented in the form of a mixed crystal. The lattice parameters and space groups of these compared with those of the room-temperature modification, are listed in Table 3. The axis of symmetry of the high-temperature structure is rotated by 90° from that of the room-temperature structure. The rotation photographs indicated a unique axis common to each cell and located such that the cell length was 0.496 nm. In the Weissenberg photographs, each unit cell shared *2 0 0* reflections. Therefore, it could be considered that the *bc* planes of the unit cell were parallel to each other and that the *ac* plane

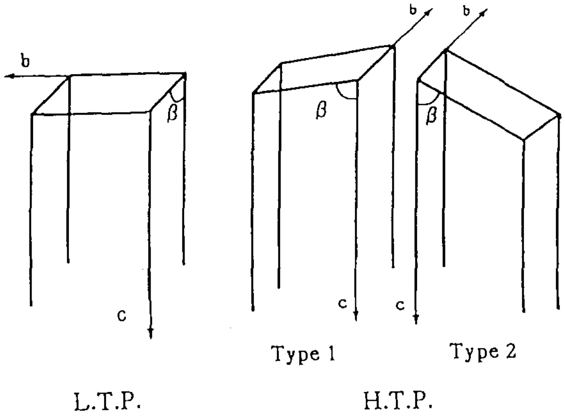

Fig. 13. Schematic representation of the unit cells for solution-crystallized sample of C52 at the high-temperature phase region.

was common as shown in Fig. 13. In the X-ray diffractions for the solution-crystallized sample of C52 at 356 K, the intensity of the Type 1 structure is weaker than that found in the crystals at 353 K. Here the temperature dependence of the long period, *L*, for C52 (the value of *L* decreased successively before melting inspite of there being only two types of high-temperature structure) was estimated as the mean value of Type 1 and Type 2 in the high-temperature structure region. It is shown therefore, that with the experimental results as stated above, Type 2 becomes more stable with increasing temperatures. It should be noted that even with the high-temperature structure, in which the thermal motion of the seems to be vigorous, the feature of the symmetry of the zigzag chain still plays a role in determining the crystalline structure.

The present X-ray investigation confirmed that the high-temperature oblique structures resemble that of the higher homologous of odd and even *n*-alkanes. As previously stated, the high-temperature phases do not seem to be unequivocally defined. The present structures may concern only the structure at the relative low temperature region. On this point, more detailed study is needed.

## 4. Conclusion

Solution-crystallized samples of henpentacontane (C51) and dopentacontane (C52) showed orthorhombic and monoclinic forms, respectively, as the stable structures at room temperature. It has, however, been recognized that the samples transform before melting to a high-temperature structure in which the end methyl plane is inclined to the chain axis. The phenomena of the freezing of the high-temperature modification (HTM) during cooling, were confirmed by the annealing of the stable crystals using DSC measurement and SEM observation. Bulk crystallized samples, therefore, with the high-temperature structures frozen-in during the cooling process did not show the peaks. It is necessary to take into consideration the existence of HTM structures when preparing samples by bulk-crystallization and studying the physical properties of samples.

X-Ray structural analysis was performed on samples grown at temperatures corresponding to HTM. The lattice parameters of C51 were determined. The C52 crystals obtained consisted of two structures simultaneously, HTM and vertical having common of *bc* and *ac* planes as well as the space grouping of $P2_1/a$.

It is interesting that the difference in molecular symmetry between C51 and C52 plays a role in determining the HTM structure, in which molecular motion seems to be vigorous and some defects are created.

## References

[1] K. Takamizawa, Y. Ogawa and T. Oyama, Polymer J., 14 (1982) 441.
[2] W. Piesczek, G.R. Stroble and K. Malzahn, Acta Crystallogr., Sect. B, 30 (1974) 1278.
[3] K. Takamizawa, Y. Nagao and Y. Urabe, Polymer J., 19 (1987) 981.
[4] K. Takamizawa, T. Sonoda and Y. Urabe, Kyushu Daigaku Sogorikogaku Kenkyuka Hokoku (Engineering Science Reports Kyushu University), 10 (1989) 363 (in Japanese).
[5] H. Wyckoff, F. Khoury and D. Hyndan, Bull. Am. Phys. Soc., 7 (1962) 207.

[6] S. Hunig, E. Lucke and E. Benzig, Chem. Ber., 91 (1958) 129.
[7] R.R. Reinhard and J.A. Dixon, J. Org. Chem., 30 (1965) 1450.
[8] F. Francis and F.J.E. Collins, J. Chem. Soc., (1936) 137.
[9] Y. Urabe and K. Takamizawa, Chem. Lett., (1992) 2315.
[10] T.K. Sullivan and J.J. Weeks, J. Res. Natl. Bur. Stand., Sect. A, 74 (1970) 203.
[11] H.M.M. Shearer and V. Vand, Acta Crystallogr., 9 (1956) 379.
[12] S.M. Ohlberg, J. Phys. Chem., 248 (1959) 248.
[13] K. Takamizawa, Y. Urabe, T. Nagano and S. Saita, unpublished work.
[14] F. Khoury, J. Appl. Phys., 34 (1963) 73.